

# Loss and revival of phase coherence in a Bose-Einstein condensate moving through an optical lattice

Francesco Nesi<sup>1,\*</sup> and Michele Modugno<sup>1,2,†</sup>

<sup>1</sup>*LENS - Dipartimento di Fisica, Università di Firenze and INFM  
Via Nello Carrara 1, 50019 Sesto Fiorentino, Italy*

<sup>2</sup>*BEC-INFM Center, Università di Trento, 38050 Povo, Italy  
(Dated: November 6, 2018)*

We investigate the phase coherence of a trapped Bose-Einstein condensate that undergoes a dynamical superfluid-insulator transition in the presence of a one-dimensional optical lattice. We study the evolution of the condensate after a sudden displacement of the harmonic trapping potential by solving the Gross-Pitaevskii equation, and comparing the results with the prediction of two effective 1D models. We show that, owing to the 3D nature of the system, the breakdown of the superfluid current above a critical displacement is not associated to a sharp transition, but there exists a range of displacements for which the condensate can recover a certain degree of coherence. We also discuss the implications on the interference pattern after the ballistic expansion as measured in recent experiments at LENS.

PACS numbers: 03.75.Kk, 05.75.Lm

## I. INTRODUCTION

The possibility of manipulating Bose-Einstein condensates (BECs) in periodic potentials has provided the opportunity to investigate a wide range of phenomena, exploring a very stimulating field which combines atomic and solid state physics [1, 2, 3, 4, 5, 6, 7, 8].

In particular, the dynamical behavior and coherence properties of BECs loaded in optical lattices have been the subject of an extensive experimental [4, 5, 6, 7, 8] and theoretical work [9, 10, 11, 12]. Recently it has been demonstrated that a trapped BEC moving through a one-dimensional optical lattice created by a laser standing wave can realize a Josephson junction array sustaining an oscillating atomic current [5]. The condensate is set in motion by a sudden displacement of the trapping potential, and then, when the center-of-mass velocity reaches a critical value, the system undergoes a transition from the superfluid regime to an insulator regime, characterized by a localization of the condensate in the trapping potential [7].

This phenomenon, which is accompanied by a loss of coherence, is triggered by the onset of a dynamical instability, as theoretically demonstrated in [9, 10, 11]. These studies rely on the analysis of the Bogoliubov spectrum of simplified one-dimensional models, and predict a sharp transition from the superfluid to the insulator regime, with a complete loss of the system coherence. Such a behavior has been confirmed in the deep insulator regime, that is for large initial displacements, by the direct solution of the three dimensional Gross-Pitaevskii equation (GPE-3D) [13].

In this work we show that, owing to the 3D character

of the system, a non-trivial phenomenology takes place in the intermediate regime where the condensate is able to retain a certain degree of coherence. The role played by the dimensionality of the system is investigated by comparing explicitly the solution of the GPE-3D with those of two one-dimensional models. We also discuss how the phase coherence of the system influences the interference pattern after the ballistic expansion, showing that the interference peaks which characterize the superfluid phase [4] are not completely destroyed in the insulator regime, though they may have a reduced visibility. The onset of decoherence processes is signaled also by additional structures (“fringes”) which appear in the central peak, as recently observed at LENS [7, 14].

The paper is organized as follows. In the next section we introduce the GPE-3D and the two one-dimensional models considered (GPE-1D and NPSE). Then, in section III we present the results by discussing the evolution of the phase coherence, the Fourier power spectrum of the system, the center-of-mass dynamics, and eventually the effect of the free expansion of the system. The conclusions are drawn in section IV.

## II. GENERAL FORMULATION

Let us consider a Bose-Einstein condensate trapped in a cylindrically symmetric harmonic potential superimposed to an optical lattice. The dynamics of the system is described by the three-dimensional Gross-Pitaevskii equation (GPE-3D) [15]

$$i\hbar \frac{\partial}{\partial t} \Psi(\mathbf{x}, t) = \left[ -\frac{\hbar^2}{2m} \nabla^2 + V(\mathbf{x}) + gN|\Psi|^2 \right] \Psi(\mathbf{x}, t) \quad (1)$$

where  $N$  is the number of condensed atoms,  $g = 4\pi\hbar^2 a/m$  the coupling strength,  $m$  the atomic mass and  $a$  the inter-atomic scattering length. The external poten-

\*Electronic address: nesi@lens.unifi.it

†Electronic address: modugno@fi.infn.it

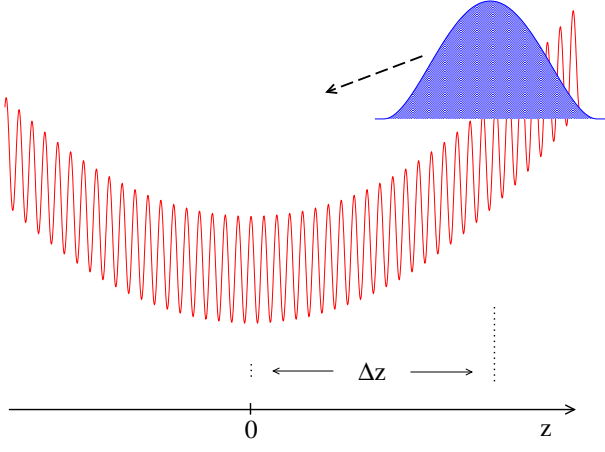


FIG. 1: Schematic of the system setup.

tial  $V(\mathbf{x}) = V_{ho}(\mathbf{x}) + V_p(z)$  is the sum of the harmonic trapping potential

$$V_{ho}(\mathbf{x}) = \frac{1}{2}m(\omega_{\perp}^2 r^2 + \omega_z^2 z^2) \quad (2)$$

and of the periodic potential generated by the optical lattice along the axial direction  $z$

$$V_p(z) = s E_r \cos^2\left(\frac{2\pi z}{\lambda}\right), \quad (3)$$

$\lambda$  being the wavelength of the laser,  $E_r \equiv \hbar^2/2m\lambda^2$  the recoil energy of an atom absorbing one lattice photon,  $d = \lambda/2$  the distance between two adjacent minima (lattice sites), and  $s$  a dimensionless parameter controlling the intensity of the lattice.

To model the LENS experiment [7], we consider a  $^{87}\text{Rb}$  condensate with  $N = 5 \cdot 10^4$  atoms, and the following parameters characterizing the external potential:  $\omega_{\perp} = 2\pi \cdot 92$  Hz,  $\omega_z = 2\pi \cdot 9$  Hz,  $\lambda = 795$  nm, and  $s = 5$ .

The ground state of the system in the combined harmonic plus periodic potential is found by mapping the wave function on a discretized grid [16] and using a standard imaginary time evolution [15]. Then, at  $t = 0$ , the harmonic potential is shifted by  $\Delta z$  and the condensate is set to evolve in the combined potentials as sketched in Fig. 1. To solve the time-dependent GPE-3D we use a split-step method which combines a FFT evolution in the axial direction [17, 18] and a Crank-Nicholson algorithm for the radial one [19].

In order to investigate the role played by the transverse dimension we also compare the full three-dimensional behavior of the GPE-3D with the solutions of two one-dimensional effective models that account for the axial dynamics along the lattice direction.

The first model considered is the 1D Gross-Pitaevskii equation (GPE-1D) given by

$$i\hbar \frac{\partial}{\partial t} \psi(z, t) = \left[ -\frac{\hbar^2}{2m} \nabla_z^2 + V(z) + g_{1D} N |\psi|^2 \right] \psi(z, t) \quad (4)$$

with

$$V(z) = \frac{1}{2}m\omega_z^2 z^2 + V_p(z) \quad (5)$$

where  $g_{1D}$  is obtained by a suitable renormalization of the 3D coupling constant  $g$ . In particular, by requiring the invariance of the Thomas-Fermi (TF) chemical potential (that is the invariance of axial size of the condensate in the TF limit) [20], we get

$$g_1 = \frac{4}{3N} \sqrt{2} \hbar \omega_z \left( \frac{\mu_{TF}}{\hbar \omega_z} \right)^{3/2} a_z \quad (6)$$

with

$$\mu_{TF} = \frac{1}{2} \hbar \omega_{\perp} \left( 15 \frac{\omega_z}{\omega_{\perp}} N \frac{a_s}{a_{\perp}} \right)^{2/5} \quad (7)$$

where  $a_z = \sqrt{\hbar/(m\omega_z)}$  and  $a_{\perp} = \sqrt{\hbar/(m\omega_{\perp})}$  are the characteristic oscillator lengths.

The other model considered here is described by the Non-Polynomial Schrödinger equation (NPSE) [21] obtained from the GPE-3D by means of a factorization of the condensate wavefunction in the product of a gaussian radial component of width  $\sigma(z, t)$ , and of an axial wavefunction  $\psi(z, t)$  that satisfies the differential equation (NPSE)

$$i\hbar \frac{\partial}{\partial t} \psi(z, t) = \left[ -\frac{\hbar^2}{2m} \nabla_z^2 + V(z) + \frac{gN}{2\pi\sigma^2} |\psi|^2 + \frac{1}{2} \hbar \omega_{\perp} \left( \frac{a_{\perp}^2}{\sigma^2} + \frac{\sigma^2}{a_{\perp}^2} \right) \right] \psi(z, t), \quad (8)$$

coupled with an algebraic equation for the radial width

$$\sigma(z, t) = a_{\perp} \sqrt[4]{1 + 2a_s N |\psi(z, t)|^2}. \quad (9)$$

Owing to this partial coupling between axial and radial degrees of freedom, the NPSE is expected, with respect to the GPE-1D, to provide a more accurate description of the actual ground-state and dynamics of the system at least in the coherent regime, as discussed in [21, 22].

### III. RESULTS AND DISCUSSION

In this section we investigate the phase coherence and the center-of-mass dynamics of the condensate during the trapped evolution through the optical lattice. To discuss the degree of coherence of the system we also show the evolution of the momentum distribution of the condensate and the expected signatures after the free expansion of the system.

#### A. Coherence

In order to characterize the degree of coherence of the condensate inside the optical lattice we define the quantity  $\chi(t)$  as the squared modulus of the correlation between values of the condensate wave function evaluated

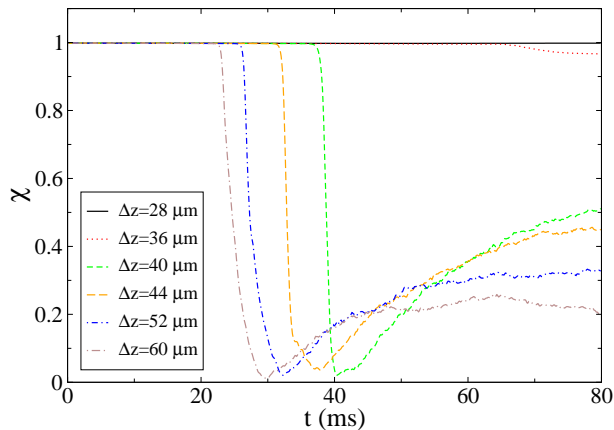


FIG. 2: Coherence of the condensate between nearest-neighbor sites of the optical lattice, obtained from the solution of the GPE-3D, for several initial displacements. After the onset of the dynamical instability (for  $\Delta z \simeq 40 \mu\text{m}$ ) the system undergoes a sudden loss of coherence, that is partially recovered for later times.

at points corresponding to the distance between nearest-neighbor sites of the lattice [10]

$$\chi(t) \equiv \left| \int d^3x \Psi^*(r, z; t) \Psi(r, z + d; t) \right|^2. \quad (10)$$

In the following we will refer to  $\chi$  as “coherence”:  $\chi = 1$  means that the system is fully coherent, whereas  $\chi = 0$  indicates a complete decoherence and the loss of the superfluid properties.

In Fig. 2 we show the evolution of the coherence for several initial displacement, up to 80 ms. The picture shows that above a critical displacement, after an initial coherent evolution, the system undergoes a sudden loss of coherence, that is partially recovered in the subsequent evolution. We have verified that for longer times (up to 200 ms) the value of  $\chi(t)$  does not grow anymore and remains close to the “saturation value” at 80 ms.

We note that even though the system may become completely incoherent ( $\chi = 0$ ), coherence is preserved in each sub-condensate (in each lattice site), and this is sufficient to justify our description of the system in terms of solutions of a differential equation.

As shown in Fig. 3 this capability of the system to regain a certain degree of coherence is due to its 3D nature. In fact, both the NPSE and the GPE-1D predict a complete dephasing after the onset of the instability, characterized by an almost vanishing coherence. The failure of these 1D effective models in the insulator regime is due to the fact that at the onset of the instability most of the energy initially associated to the coherent evolution of the system is absorbed by the modes responsible for the dynamical instability, which grow exponentially in time destroying the phase coherence of the condensate [9, 10]. However, while in the 1D case all the energy is transferred to these modes, in the 3D case the interplay between radial and axial degrees of freedom, coupled through the

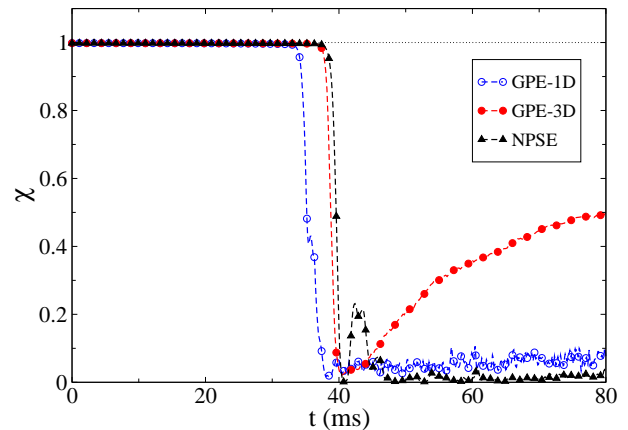


FIG. 3: Coherence of the condensate between nearest-neighbor sites of the optical lattice for a displacement  $\Delta z = 40 \mu\text{m}$ . When the system enter the insulator regime the 1D models (GPE-1D, empty circles; NPSE, triangles) predict a complete loss of coherence, while the actual (3D) behavior of the system is characterized by a partial recover of coherence (GPE-3D, filled circles).

nonlinear term, allows for a partial transfer of energy to coherent modes of the condensate, acting, as a matter of fact, as a restraint to the decoherence process [24]. Note in this respect that the partial coupling between axial and radial degrees of freedom in the NPSE is not sufficient to account for the rephasing mechanism, and this is likely due to the simple gaussian factorization of the wave-function which produces a coupling just between radial and axial densities [21], losing any information on the phase dynamics [25].

## B. Center-of-mass dynamics

Let us now discuss the center-of-mass evolution along the lattice direction, by considering the axial coordinate

$$z_{cm}(t) = \int d^3x z |\Psi(r, z; t)|^2, \quad (11)$$

and its velocity

$$v_{cm}(t) = \frac{\hbar}{2im} \int d^3x [\Psi^* \nabla_z \Psi - \Psi \nabla_z \Psi^*]. \quad (12)$$

In Fig. 4 we show the evolution of  $v_{cm}(t)$  during the trapped dynamics, for several initial displacements (see also Fig. 2). This picture points out clearly the existence of a critical velocity independent of the initial displacement (here  $|v_{crit}| \simeq 1.25 \text{ mm/s}$ , in nice agreement with the experimental value reported in [7]), beyond which the system cannot sustain a coherent oscillation. This is due to the presence of axial modes with imaginary frequency that grow exponentially in time and are responsible for the dynamical instability of the system in a certain range of condensate quasimomenta [9, 10].

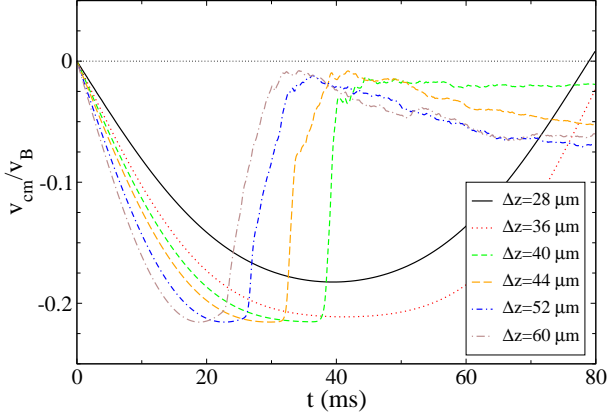


FIG. 4: Center-of-mass velocity of the condensate (in units of the Bragg velocity  $v_B = \hbar\pi/(md)$ ) obtained from the solution of the GPE-3D, for several initial displacements. This picture clearly shows that the decoherence process is characterized by the achievement of a critical velocity (see also Fig. 3).

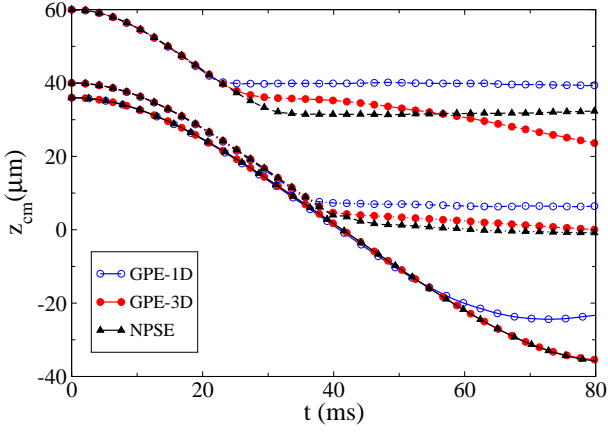


FIG. 5: Center-of-mass dynamics for three values of the initial displacement ( $\Delta z = 36 \mu\text{m}$  continuous line,  $\Delta z = 40 \mu\text{m}$  dashed-dotted,  $\Delta z = 60 \mu\text{m}$  dashed). Contrarily to what happens in the simplified 1D models (GPE-1D, empty circles; NPSE, triangles), in the insulator regime the condensate center-of-mass continues a slow evolution toward the center of the trap (GPE-3D, filled circles).

In Fig. 5 we compare the corresponding center-of-mass evolution with the prediction of the one-dimensional models, for three initial displacements. We notice that the GPE-3D predicts a slow motion toward the center of the trapping potential, as observed in the experiment [7, 14], whereas the 1D models predict a sudden localization of the system as a consequence of the complete loss of coherence.

Note also that for small initial displacements, that is in the regime of coherent oscillations, the predictions of the NPSE are in nice agreement with those obtained by the full GPE-3D, while the GPE-1D deviates from the expected behavior after about 40 ms of evolution (we have observed in a similar fashion that the GPE-1D slightly

underestimates the critical displacement). This effect may be due to the chosen renormalization of the coupling constant  $g_1$  (see Eq. (6)) that can overestimate non-linear effects [22] responsible for the existence of dynamically unstable modes. However, even though one tunes  $g_1$  in order to better reproduce the actual critical displacement, this would not change the inadequateness of the model to describe the behavior of the system in the insulator regime, neither the fact that in any case the NPSE represents a more reliable effective model (with respect of the “simple” GPE-1D) to describe the dynamics of the system in the superfluid regime [21, 22].

### C. Momentum evolution

Let us now consider the evolution of the axial momentum density distribution (power spectrum), which provides a deeper understanding of the system behavior and of the dephasing mechanisms. In Figs. 6 and 7 we show the axial power spectrum of the condensate, defined as

$$P(p_z) \equiv 2\pi \int r dr |\tilde{\Psi}(r, p_z)|^2 \quad (13)$$

(the tilde indicates the Fourier transform along  $z$ ), in the case of an initial displacement  $\Delta z = 40 \mu\text{m}$ , at subsequent evolution times. In particular, in Fig. 6 we consider three configurations when the condensate is still in the superfluid regime, respectively for  $t = 0$  ms (a), 15 ms (b) and 30 ms (c). In this case the power spectrum is characterized by sharp peaks localized at  $\tilde{p}_z(t) = \pm 2np_B + q(t)$  ( $n = 0, \pm 1, \dots$ , here only the zero and first order are visible) [4],  $p_B = mv_B = \hbar\pi/d$  being the Bragg momentum and  $q(t)$  the condensate quasimomentum. In fact, when the lattice intensity is sufficiently high (i.e. we are in the *tight binding* regime), the condensate in a Bloch state of quasimomentum  $q$  can be written as [23] (neglecting for simplicity the presence of the harmonic potential which breaks the periodicity of the lattice [26])

$$\Psi(r, z) = \sum_k e^{-iqkd} \varphi(r, z + kd) \quad (14)$$

where  $\varphi(r, z + kd)$  are wave functions localized at each lattice site (labeled by the index  $k$ ). It is straightforward to show that in the coherent regime the momentum distribution is characterized by sharp peaks whose weight is modulated by the axial Fourier transform of the wave function at each lattice site [4]

$$P_q(p_z) = \frac{\sin^2(N_l(p_z - q)d/2\hbar)}{\sin^2((p_z - q)d/2\hbar)} 2\pi \int r dr |\tilde{\varphi}(p_z, r)|^2 \quad (15)$$

$N_l$  being the number of occupied lattice sites [4].

Contrarily, the behavior of the system in the insulator regime is completely different, as shown in Fig. 7 for  $t = 45$  ms (a), 60 ms (b), and 80 ms (c). Indeed, after the onset of the dynamical instability, the momentum

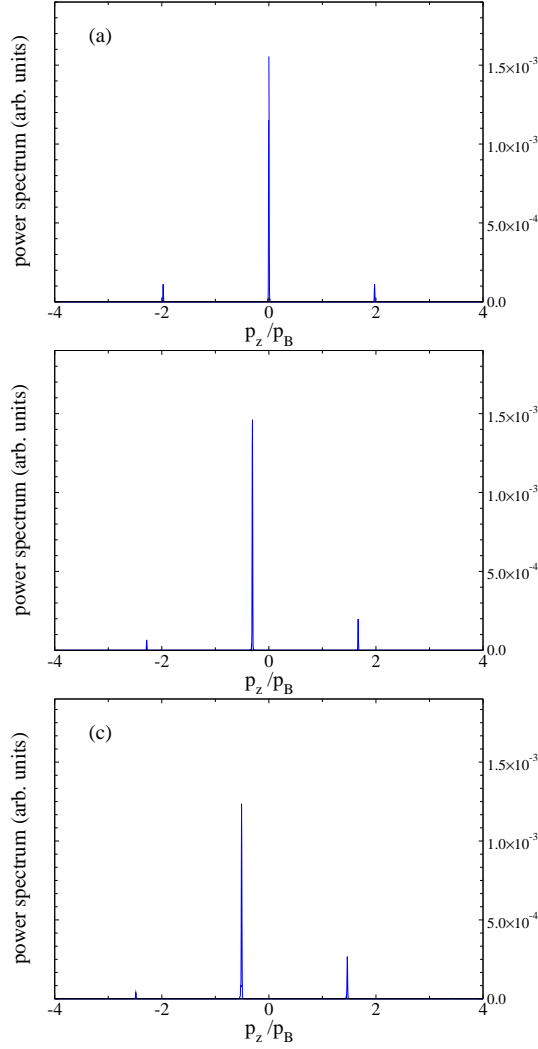


FIG. 6: Axial power spectrum of the condensate in the superfluid regime for  $t = 0$  ms (a), 15 ms (b) and 30 ms (c). The presence of sharp peaks spaced apart by multiples of  $\pm 2p_B$  is a signature of the system coherence [4].

distribution initially spreads out losing any signature of coherence (Fig. 7(a)). Afterwards, the system tries to rearrange itself in a coherent fashion as signaled by the appearance of structures localized in correspondence of the initial peaks. Even though these “peaks” have a rather large spread (see Fig. 7(c)), the relative population with respect to the central one is of the same order of that in the full coherent regime (Fig. 6(a)). Notice also that the momentum distribution is centered not exactly in  $p_z = 0$  since the condensate is slightly moving toward the trap center.

For comparison, in Fig. 8 we show the axial power spectrum as obtained from the NPSE, after an evolution of 80 ms. In this case there is no evidence of any localized structure (contrarily to the case of Fig. 7(c)) as further confirmation of the fact that these effective one-dimensional models cannot account for an accurate

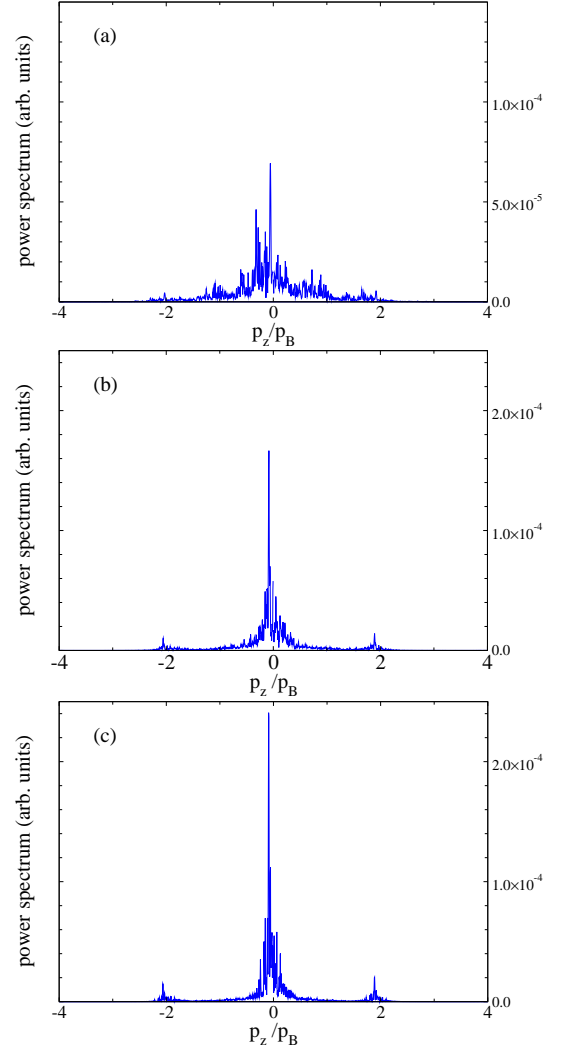


FIG. 7: Axial power spectrum of the condensate in the insulator regime for  $t = 45$  ms (a), 60 ms (b), and 80 ms (c).

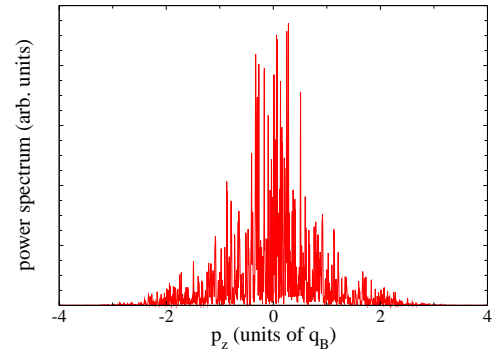


FIG. 8: Axial power spectrum of the NPSE solution after an evolution of 80 ms. The distribution is completely spread out indicating a complete loss of coherence.

description of the system behavior in the insulator regime (similar considerations hold for the GPE-1D).

#### D. Free expansion

In this section we discuss the expected behavior of the system after a ballistic expansion. When the system is in the superfluid regime the internal coherence of the condensate shows up in a clear interference pattern characterized by lateral peaks that move outwards at velocities  $v = \pm 2p_B/m$  [4]. Contrarily, in the insulator regime we expect the overall shape of the interference pattern and also the expansion of the central peak to be affected by the partial loss of coherence, as we will show in the following.

To investigate these aspects, instead of solving the full GPE-3D, we use a simplified model in order to avoid unnecessary heavy numerical computations [27]. In particular, since we are mainly interested in the expanded axial profile, we neglect the contribution of the mean field interaction, and we assume a free expansion governed by the Schrödinger equation

$$i\hbar \frac{\partial}{\partial t} \Psi(r, z; t) = -\frac{\hbar^2 \nabla^2}{2m} \Psi(r, z; t). \quad (16)$$

The reason to use this approximation is threefold.

(i) First of all, in our case most of the initial energy of the condensate (at the moment of the release from the trap) is associated to the fast density modulation, due to the presence of the optical lattice. Therefore, contrarily to “usual” case of a pure harmonic confinement, now the kinetic energy term predominates over the mean field one,  $E_{mf} \ll E_{kin}$ .

(ii) Another reason is that we expect the mean-field interaction to affect mainly the radial expansion, which is however integrated out in our treatment.

(iii) Finally, since our aim is to investigate the overall shape of the interference pattern and to point out the possible presence of lateral peaks (and/or other signatures of the degree of coherence of the system) rather than the exact size of the central peak, we can for this purpose neglect the contribution of the mean field term [22].

Then, by using Eq. (16) it is easy to show that the axial density distribution after an expansion time  $t_{exp}$  is given by ( $\hbar = 1$ )

$$\begin{aligned} \rho(z; t_{exp}) &\equiv \int d^2r |\Psi(r, z; t_{exp})|^2 \\ &= \int d^2r \left| \int dp_z e^{ip_z z} \tilde{\Psi}_0(r, p_z) e^{-i(p_z^2/2m)t_{exp}} \right|^2, \end{aligned} \quad (17)$$

$\tilde{\Psi}_0(r, p_z)$  being the axial Fourier transform of the initial wave function (at the time of the release from the trap).

As an example in Fig. 9 we show the typical shape of the density distribution before (a) and after (b) an expansion of about 30 ms, corresponding to a case similar

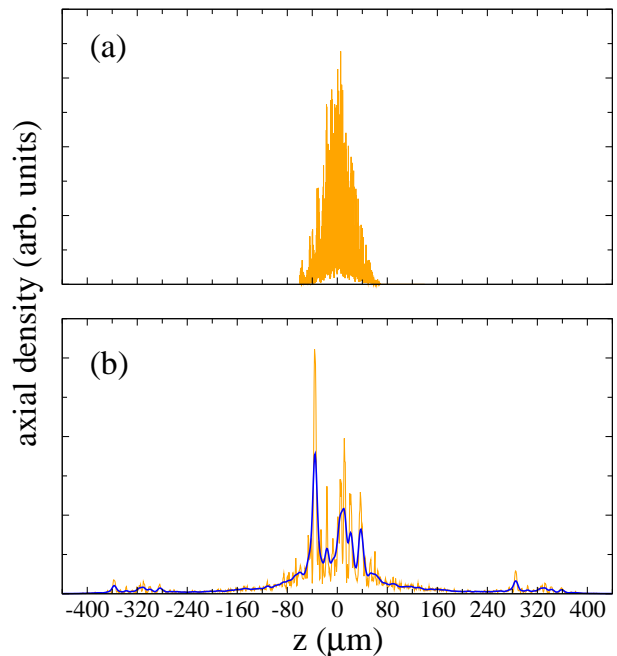


FIG. 9: (a) Axial profile of the condensate in the trap, in the insulator regime (for a displacement  $\Delta z = 40 \mu\text{m}$  and after 70 ms of trapped evolution). (b) Interference pattern (lateral peaks) and fringes (in the central peak) after a subsequent expansion of about 30 ms. The marked line in (b) is obtained by taking into account the finite resolution of the imaging apparatus as described in the text.

to those in Figs. 7(b)-(c). We see that both distributions are characterized by a rather fragmented profile, although after the expansion (Fig. 9(b)) it is possible to identify some structures localized in correspondence of the first order peaks of the analogous expanded profile in the case of a fully coherent condensate (at  $z \simeq 320 \mu\text{m}$ ) [4].

Furthermore, to take into account the effect of the finite resolution of the experimental imaging apparatus, in Fig. 9(b) we also show the convolution (marked line) of the axial density with a gaussian distribution of width  $\sigma$  (here  $2\sigma = 6 \mu\text{m}$ , according to the typical experimental resolution). This procedure clearly evidences the persistence of lateral peaks and the appearance of fringes in the central one, whose presence is a signature of the partial loss of coherence (as the reduced visibility of the lateral peaks).

Note that although the actual shape of the interference pattern depends on the initial conditions (as for example the trapped evolution time), the overall behavior shown in Fig. 9(b) can be reproduced for a wide range of trap displacements and evolution/expansion times. We have also verified that the main features discussed in this work hold for lattice intensities in the range  $2 < s < 10$ .

Both the persistence of the lateral peaks and the appearance of fringes in the central peak in the density distribution of the expanded condensate have been recently



observed in the experiments at LENS [7, 14].

#### IV. CONCLUSIONS

We have studied the phase coherence of a Bose-Einstein condensate that undergoes a dynamical superfluid-insulator transition during the trapped evolution in the presence of a one-dimensional optical lattice, as recently observed at LENS [7, 14] and discussed in [9, 10, 13].

From the comparison of the solution of the three-dimensional Gross-Pitaevskii equation with that of two effective 1D models, we have demonstrated that the inclusion of the transverse degrees of freedom is crucial to account for the actual behavior of the system, as observed in the experiments [7, 14]. In particular we have shown that the breakdown of the superfluid current is not associated to a sharp transition as predicted for the pure one-dimensional case, but there exists a range of parameters for which the condensate can partially recover some

coherence during the subsequent evolution.

We have also shown that the degree of coherence of the system affects significantly the interference pattern after the ballistic expansion of the condensate, characterized by the persistence of lateral peaks (as a signature of a partial coherence) and by the appearance of fringes in the central peak (due to the dephasing of the system).

These results open interesting questions about the precise role played by the radial degrees of freedom on the excitation spectrum and on the decoherence mechanism. The investigation of these aspects requires the analysis of the 3D Bogoliubov spectrum of the system, and will be addressed in a future publication.

#### Acknowledgments

We acknowledge stimulating discussions with F. Dalfovo, L. Pitaevskii and C. Fort.

- 
- [1] B. P. Anderson and M. A. Kasevich, *Science* **282**, 1686 (1998).
  - [2] C. Orzel, A. K. Tuchman, M. L. Fenselau, M. Yasuda and M. A. Kasevich, *Science* **291**, 2386 (2001).
  - [3] M. Greiner, O. Mandel, T. Esslinger, T. W. Hänsch and I. Bloch, *Nature* **415**, 39 (2002).
  - [4] P. Pedri, L. Pitaevskii, S. Stringari, C. Fort, S. Burger, F. S. Cataliotti, P. Maddaloni, F. Minardi and M. Inguscio, *Phys. Rev. Lett.* **87**, 220401 (2001).
  - [5] F. S. Cataliotti, S. Burger, C. Fort, P. Maddaloni, F. Minardi, A. Trombettoni, A. Smerzi and M. Inguscio, *Science* **293**, 843 (2001).
  - [6] S. Burger, F. S. Cataliotti, C. Fort, F. Minardi and M. Inguscio, M. L. Chiofalo and M. P. Tosi, *Phys. Rev. Lett.* **86**, 4447 (2001); B. Wu and Q. Niu, *Phys. Rev. Lett.* **89**, 088901 (2002); S. Burger, *et al.*, *Phys. Rev. Lett.* **89**, 088902 (2002).
  - [7] F. S. Cataliotti, L. Fallani, F. Ferlaino, C. Fort, P. Maddaloni and M. Inguscio, *New J. Phys.* **5**, 71 (2003).
  - [8] O. Morsch, J.H. Müller, M. Cristiani, D. Ciampini, and E. Arimondo, *Phys. Rev. Lett.* **87**, 140402 (2001).
  - [9] B. Wu and Q. Niu, *Phys. Rev. A* **64**, 061603 (2001); *cond-mat/0306411*.
  - [10] A. Smerzi, A. Trombettoni, P. G. Kevrekidis and A. R. Bishop, *Phys. Rev. Lett.* **89**, 170402 (2002).
  - [11] M. Machholm, C. J. Pethick, and H. Smith, *Phys. Rev. A* **67**, 053613 (2003); M. Machholm, A. Nicolin, C. J. Pethick, and H. Smith, *cond-mat/0307183*.
  - [12] V. Konotop, and M. Salerno, *Phys. Rev. A* **65**, 021602 (2002).
  - [13] S. K. Adhikari, *Eur. Phys. J. D* **25**, 161 (2003); *cond-mat/0308085*; *cond-mat/0308415*.
  - [14] F. S. Cataliotti, L. Fallani, C. Fort, and M. Inguscio, private communication.
  - [15] F. Dalfovo, S. Giorgini, L. P. Pitaevskii, S. Stringari, *Rev. Mod. Phys.* **71**, 463 (1999).
  - [16] For the numerical grid we use up to 64 sites in the radial direction and 8192 in the axial one (the direction of the lattice).
  - [17] W. H. Press *et al.*, *Numerical Recipes* (Cambridge University Press, N.Y. 1986-92).
  - [18] B. Jackson, J. F. McCann and C. S. Adams, *J. Phys. B* **31**, 4489 (1998).
  - [19] F. Dalfovo and M. Modugno, *Phys. Rev. A* **61**, 023605 (2000); A. Brunello, F. Dalfovo, L. Pitaevskii, S. Stringari and F. Zambelli, *ibid.* **64**, 063614 (2001).
  - [20] M. Trippenbach, Y. B. Band and P. S. Julienne, *Phys. Rev. A* **62**, 023608 (2000).
  - [21] L. Salasnich, *Laser Physics* **12**, 198 (2002); L. Salasnich, A. Parola and L. Reatto, *Phys. Rev. A* **65**, 043614 (2002).
  - [22] P. Massignan and M. Modugno, *Phys. Rev. A* **67**, 023614 (2003).
  - [23] N. W. Ashcroft and N. D. Mermin, *Solid State Physics* (Saunders College, Philadelphia 1976).
  - [24] The investigation of actual mechanism which determines this behavior deserves a deeper investigation that goes beyond the scope of this work.
  - [25] In the case of coherent excitations, and also for a free expansion, it is possible to use a more reliable ansatz as discussed in Ref. [22]
  - [26] This assumption is justified by the fact that the condensate extends over many lattice sites, due to the weak trapping along the axial direction.
  - [27] In principle one should solve the full GPE-3D on a grid large enough to describe the evolution of the peaks moving outwards with velocity  $\pm 2p_B/m$ .